



Chromium picolinate attenuates cognitive deficit in ICV-STZ rat paradigm of sporadic Alzheimer's-like dementia via targeting neuroinflammatory and IRS-1/PI3K/AKT/GSK-3 β pathway

Ansab Akhtar¹ · Jatinder Dhaliwal¹ · Priyanka Saroj¹ · Ankit Uniyal¹ · Mahendra Bishnoi² · Sangeeta Pikhwal Sah¹ 

Received: 31 October 2019 / Accepted: 16 December 2019 / Published online: 3 January 2020
© Springer Nature Switzerland AG 2020

Abstract

Alzheimer's disease (AD) is prevalent in old age people and is one of the most common brain diseases. Brain insulin resistance, neuroinflammation, oxidative stress, and mitochondrial and cholinergic dysfunction are key features of the disease. In our study, streptozotocin (STZ) in a dose of 3 mg/kg was injected in male Wistar rats bilaterally through the intracerebroventricular (ICV) route on stereotaxic apparatus. Chromium picolinate (CrPic) was tested at doses of 1 mg/kg, 2 mg/kg, and 4 mg/kg, while rivastigmine (2 mg/kg) was used as reference standard drug. Cognitive dysfunction induced by STZ was assessed by behavioral tests like Morris water maze and novel object recognition test. Treatment with CrPic revealed attenuation of cognitive deficit. This was confirmed by behavioral tests, biochemical estimations of antioxidant enzymes, oxidative stress, nitrosative stress, and cholinergic and mitochondrial activity. CrPic did not change AchE activity significantly. STZ-induced neuroinflammation evident by increased TNF- α , IL-6, and CRP levels was also significantly decreased by CrPic. Dysfunctional insulin signaling after ICV-STZ was demonstrated by reduced IRS-1, PI3K, AKT, BDNF gene expression, and increased GSK-3 β , NF- κ B gene expression with the help of qRT-PCR. CrPic treatment produced an improvement in insulin signaling revealed by increased gene expression of IRS-1, PI3-K, AKT, BDNF, and decreased gene expression of GSK-3 β and NF- κ B. It was concluded that CrPic reversed AD pathology revealed by improved memory, reduced oxidative stress, neuroinflammation, mitochondrial dysfunction, and upregulated insulin signaling.

Keywords ICV-STZ · Chromium picolinate · Oxidative stress · Neuroinflammation · Insulin resistance · Alzheimer's disease

✉ Sangeeta Pikhwal Sah
spikhwal@rediffmail.com

Ansab Akhtar
ansabakhtar@gmail.com

Jatinder Dhaliwal
jatinderdhaliwal57@yahoo.com

Priyanka Saroj
priyanka1960@gmail.com

Ankit Uniyal
ankituniyal1994rsb@gmail.com

Mahendra Bishnoi
mbishnoi@gmail.com

¹ Pharmacology Division, University Institute of Pharmaceutical Sciences, Panjab University, Chandigarh 160014, India

² National Agri-Food Biotechnology Institute (NABI), Sector-81, SAS Nagar, Mohali, Punjab 140306, India

Introduction

Alzheimer's disease (AD) is one of the most common forms of dementia affecting elderly people. People suffering from AD show symptoms of cognitive impairment, memory deficit, and disturbances in behavioral activities (Onor et al. 2006). According to the 2017 report, around 44 million people globally are suffering from AD with disease prevalence likely to rise to 115 million by 2050 (Sargent and Brown 2017).

Despite more than 30 years of intense investigation, the field lacks consensus regarding the etiology and pathogenesis of sporadic AD, and therefore, we still do not know the best strategies for treating and preventing this debilitating disease. Moreover, the prevalence of AD is increasing rapidly in the absence of truly effective therapies. Epidemiologic studies in elderly, experimental investigations in humans and animal models consistently demonstrate that

dysfunctional brain insulin signaling termed brain insulin resistance promotes and accelerates cognitive dysfunction and AD progression. This might be responsible for the sporadic and age-related AD (Talbot et al. 2012).

Insulin signaling impairment and irregularities in its molecules are found to be involved in AD characterized by impaired memory and cognitive dysfunction (Steen et al. 2005). PI3K and AKT facilitate the transfer of GLUT 1 and GLUT 3 glucose transporters stimulating glucose uptake inside brain cells (Deng et al. 2009). Therefore, insulin-mediated activation of PI3K/AKT pathway enhances glucose and energy metabolism in the brain. In AD, there is a hindrance in the binding of insulin to its receptors, resulting in dysregulated insulin signaling (Frölich et al. 1999). Moreover, AD has been demonstrated to show reduced sensitivity to insulin signaling in the IRS-1/PI3K pathway (Talbot et al. 2012). Reduced insulin sensitivity was found to be highest at the IRS-1 level (Talbot et al. 2012). Furthermore, decreased activation of PI3K/AKT leads to increased activation of GSK-3 β , which is responsible for increased tau phosphorylation as well as augmented amyloid plaques deposition, the two major pathological hallmarks of AD (Baki et al. 2004). Most importantly, a positive association between increased GSK-3 β mRNA gene expression and tau phosphorylation has been reported (Del Pino et al. 2016).

Insulin shows neuromodulatory actions in the brain and insulin signaling is involved in neuronal survival, energy production, gene expression, and neuronal plasticity. Brain insulin resistance, neuroinflammation, and oxidative stress promote A β toxicity and formation of neurofibrillary tangles (de la Monte 2012).

Chromium is defined as a trace element supplemented either with food or water. It is absorbed less than 3% from the intestine. The salt, chromium picolinate (CrPic) is, however, highly absorbed (Anderson et al. 1996). The natural sources of chromium include potatoes, tomatoes, oysters, broccoli, grape juice, and seafood, etc. CrPic has been studied to improve insulin sensitivity in diabetes mellitus (DM) by targeting the IRS-1/PI3K/AKT/GSK-3 β pathway (Martin et al. 2006; Hua et al. 2012). CrPic binds to insulin receptor increasing tyrosine kinase activity, and hence, the downstream molecules such as AKT/PI3K are activated and GSK-3 β is subsequently inactivated (Desbois-Mouthon et al. 2001; Hua et al. 2012). Chromium salt has been proved to ameliorate diabetic symptoms by increasing the levels of antioxidant enzymes (Anderson et al. 2001). The antioxidant and anti-inflammatory activities of CrPic are mediated through Nrf2 and NF κ B pathway, by increasing and decreasing their activities, respectively (Sahin et al. 2012; Selcuk et al. 2012). CrPic was found to be non-toxic in rats weighing 200–250 gm even after 3 mg consumption daily for 20 weeks (Franklin and Odontiadis 2003). Previous studies also support the protective effect of chromium picolinate in

depression, anxiety (Dubey et al. 2015), and diabetic brain (Sahin et al. 2012).

However, to date, the neuroprotective effects of CrPic remain to be investigated in AD. Therefore, in the present study, we investigated the primary effect of CrPic by targeting IRS-1/PI3K/AKT/GSK-3 β pathway of insulin signaling in the ICV-STZ model of AD which closely mimics insulin signaling impairment and insulin resistance.

Materials and methods

Animals

Male Wistar rats (210–280 g) of 8–10 weeks of age were acquired from Central Animal House, Panjab University, Chandigarh. Rats were housed in a pathogen-free environment. Animals were kept in polypropylene breeding cages containing paddy husk bedding. Food and water were given regularly. The habitation of animals was done for 3–4 months at 12 h alternate dark/light cycles, and temperature maintained at 25 ± 5 °C irrespective of the outside weather. Normal humidity of the room for animals was $55 \pm 10\%$. All the experiments were carried out between 9 a.m. and 5 p.m. in a controlled environment.

Guidelines of Committee for the Purpose of Control and Supervision of Experiments on Animals (CPCSEA) were followed during the whole process of experimental work. The study protocol was approved by the Institutional Animal Ethics Committee (IAEC) with approval no: PU/45/99/CPCSEA/IAEC/2018/99.

Drugs and chemicals

Streptozotocin (STZ) (CAS No.18883-66-4) was purchased from SRL Pvt. Ltd. India. Chromium picolinate (CrPic) was purchased from Research Lab Fine Chem Industries, Mumbai, India. Rivastigmine tartrate was purchased from Sun Pharma Laboratories Ltd. STZ was given in artificial CSF (2.9 mM KCl, 147 mM NaCl, 1.7 mM CaCl₂, 1.6 mM MgCl₂, and 2.2mMD-glucose). Ketamine and xylazine were injected as a cocktail. The doses of CrPic (Mozaffari et al. 2005; Sundaram et al. 2013; Dubey et al. 2015) and rivastigmine (Sachdeva et al. 2014) were decided based on previously reported studies. All the solutions were freshly prepared and all the chemicals used were of analytical grade.

Experimental animal groups and protocol design

Adult male Wistar rats ($n = 64$) were selected and randomly divided into eight groups comprising of eight animals in each group. Behavioral tests, and biochemical and molecular estimations were performed as per the experimental design

(Fig. 1). All the treatments to the animals were started from 9:30 a.m. every day in the experimental laboratory during the whole experimental protocol.

Group 1 Normal control animals referred to as naive animals received distilled water by oral gavage for 21 days, starting from day 1, i.e., on the next day of surgery of other parallel groups. Although, surgery was not performed in this group.

Group 2 Sham control animals were injected with ICV-artificial cerebrospinal fluid (aCSF) in a volume of 4 μ l bilaterally by surgical procedure on a stereotaxic apparatus and received distilled water by oral gavage for 21 days, starting from day 1, i.e., on the next day of surgery.

Group 3 Negative control animals were injected with ICV-STZ dissolved in aCSF (3 mg/kg, 4 μ l) bilaterally on a stereotaxic apparatus and received distilled water by oral gavage for 21 days, starting from day 1, i.e., on the next day of surgery.

Group 4 ICV-STZ-induced animals were given the lowest dose (1 mg/kg) of the test drug, i.e., CrPic by oral gavage for 21 days, starting from day 1, i.e., on the next day of surgery.

Group 5 ICV-STZ-induced animals were given the medium dose (2 mg/kg) of CrPic by oral gavage for 21 days, starting from day 1, i.e., on the next day of surgery.

Group 6 ICV-STZ-induced animals were given the highest dose (4 mg/kg) of Cr.Pic by oral gavage for 21 days, starting from day 1, i.e., on the next day of surgery.

Group 7 ICV-STZ-induced animals were treated with rivastigmine (2 mg/kg) by oral gavage for 21 days, starting from day 1, i.e., on the next day of surgery. This group was referred to as positive control where rivastigmine acted as reference standard drug.

Group 8 In the per se group, no stereotaxic surgery was performed and no ICV-STZ was administered. The highest dose of CrPic (4 mg/kg) was given by oral gavage for 21 days starting from day 1, i.e., on the next day of surgery.

Intracerebroventricular streptozotocin administration through stereotaxic surgery

Streptozotocin was administered intracerebroventricularly in rats using a stereotaxic apparatus. Rats were anesthetized with ketamine (60 mg/kg, i.p.) + xylazine (10 mg/kg, i.p.). The head was shaved and then positioned in a stereotaxic frame, so that the scalp is tightened and straight. A mid-line sagittal incision was made on the scalp with a sharp scalpel blade. Bregma was located by removing the layer of connective tissue over the skull and cleaned with saline.

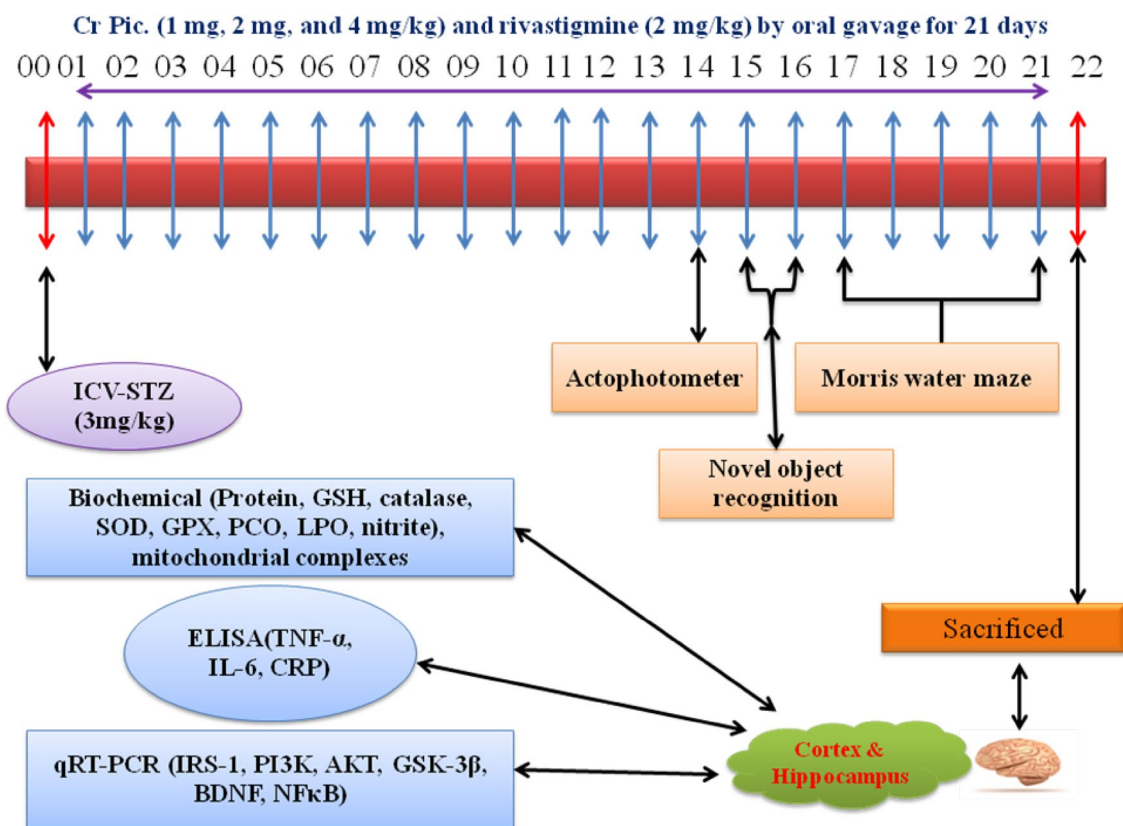


Fig. 1 Experimental design

Coordinates such as 0.8 mm posterior to bregma, 1.5 mm lateral to sagittal suture on both left and right sides, and 3.6 mm beneath the surface of the skull were adjusted digitally. A burr hole was drilled with a driller through the skull on both sides over the lateral ventricle taking care that no blood leaks out. Microlitre Hamilton syringe was filled with STZ or aCSF up to 8 μ l mark. Bilateral injection of STZ (3 mg/kg) dissolved in aCSF was slowly administered in a volume of around 4 μ l on each side with a speed of almost 1 μ l/min. While administration, the syringe was kept fully upright. After delivering, it was kept as such for 1–2 min to evade expulsion of the injectable substance. The animal was then taken out of the apparatus. Within 1–2 min, dental cement and fixer were applied over the injected place to fill the drilled hole, which is then removed after cement gets dried. The incised skin was stitched with black surgical thread and suturing needle, followed by the application of betadine over it. Saline was applied to the eyes to avoid dryness. Betadine and antiseptic were applied over the stitched area for 3–4 days to combat infection. Sham group animals received the same volume of aCSF and the same procedure was followed (Sharma and Gupta 2002).

Behavioral assessments

Close field activity (CFA)

On day 14, in an actophotometer, locomotor or closed field activity was determined. Actophotometer is a square box-shaped ($30 \times 23 \times 22$ cm³) arena, enclosed from all the sides and a lid on the top of it. It comprises of 16 infrared photocells on the front side of the chamber, 8 each at a height of 3 cm and 9 cm, respectively (IMCORP, Ambala, India). For the assessment of locomotor activity, rats were first acclimatized for 2–3 min inside the chamber, and then, the photocell counter was switched on to record the readings for ambulation and rearing. The light from the photocell was cut when the animal comes across it and the counts of readings were recorded automatically. For the record of reading, each animal was kept in the actophotometer for 5 min., and ambulatory as well as rearing scores were noted down. After taking off the animal from the chamber, the floor was cleaned with 70% ethanol. The scores for both ambulations and rearings were counted to determine the locomotor activity (Sachdeva et al. 2014).

Novel object recognition (NOR)

NOR was performed on days 15 and 16 to determine the recognition or associative memory by evaluating the recognition or discrimination ability of rats for two different objects (Antunes and Biala 2012). In a circular open field of diameter 50 cm and a wall of height 40 cm, with moderate

daylight, training of the rats was done for 2–3 min on day 15. Rats were habituated and familiarized with the area. On the same day, another training was done with two similar objects of 10 cm height, rectangular in shape, red color cap, and white color body with a smooth texture. Objects were kept and fixed with tape on the floor of the arena at a distance of 10 cm from the wall. The two objects were distanced by almost 20 cm from each other. Each animal was put in the circular arena facing the head towards the wall and kept for 5 min to explore and get familiarized with the two similar objects. Exploration of the objects was considered when the animals directed the nose towards the object at a distance less than or equal to 2 cm, sniffed the object, or touched the object while looking at it. The whole process was video recorded. The animal was taken off from the arena. The whole areas, as well as the objects, were cleaned with 70% ethanol to exclude the olfactory cues for the animals.

On the next day, i.e., day 16, one familiar object was replaced with a novel object of round shape, grey color, rough texture, and the almost same height of the familiar object. This novel object was kept at the same place and fixed in the same way as the earlier familiar object. Video recording of animals was done, while they were exploring the objects. While counting the exploration time, the experimenter was blind to the treatments of the rats. Time to explore the familiar and novel object was determined. Discrimination index (DI) was calculated according to the following formula (Antunes and Biala 2012):

$$DI = (T_n - T_f) / (T_n + T_f).$$

Here, T_n and T_f represent the time to explore the novel and familiar object, respectively.

Morris water maze (MWM)

MWM was performed for 5 days on days 17–21 for the evaluation of spatial learning and memory (Morris et al. 1982). The training period lasted for 4 days followed by probe trial on the 5th day of MWM.

MWM is a circular tank having dimensions of 180 cm diameter and 60 cm height. The whole tank was divided into four quadrants by two white threads tied over the top brim of the tank. In one of the quadrants, a square-shaped platform of area 12 cm² and a height 38 cm was kept. The tank was filled to almost 2/3rd with water (28 ± 2 °C) to hide the platform just 2 cm below the water surface to make it invisible to rats. The platform was kept in the fourth quadrant referred to as the target quadrant. Rats were trained for 4 days to navigate the hidden platform. These trainings were done by putting the rat in each of the quadrants starting from the first quadrant. While putting, the face of the animals was kept towards the wall of the tank and the starting location was

chosen close to the wall. The wall is marked with different signs and colors on each quadrant as a clue for animals to navigate and locate the platform. A total of four trials were done for each animal in each quadrant for 4 days.

For the trial, rats were allowed to swim for 90 s, taken as cut-off time. If the animal could not locate the platform in 90 s, then it was guided to the platform manually with a wooden stick. The animal was left on the platform for 15 s before returning it to the home cage. If the animal finds the platform in 90 s or less than 90 s, then that time was counted as escape latency. This parameter was noted down for the first 4 days of the trial.

While performing the probe trial on the final day, i.e., on the 5th day of MWM, the platform was taken off from the tank. The probe trial was done for 60 s for each animal and in all the four quadrants. The parameters assessed were time spent in the target quadrant (TSTQ) and the number of entries in the target quadrant (NETQ) (Morris 1984).

Biochemical assessments

Homogenization of cortex and hippocampus

On day 22, animals were anesthetized with ketamine (60 mg/kg, i.p.) + xylazine (10 mg/kg, i.p) followed by decapitation. The brain was immediately removed, and the tissues of cortex and hippocampus were dissected on an ice plate. All the tissues were divided into two halves, washed with ice-cold PBS, and immediately stored at -80°C for 2–3 days. The entire animal tissues in each group were again randomly grouped into two sets. One set of already halved tissues were processed for biochemical and mitochondrial estimations, and the second set of halved tissues were processes for ELISA and qRT-PCR. Later, tissues were homogenized in a chilled phosphate buffer (pH 7.4). The white-colored thick homogenate was obtained which was then centrifuged at 10,000g at 4°C for 20 min. The supernatant was collected for assessment of biochemical parameters, mitochondrial activity, and ELISA. Hippocampal tissues for qRT-PCR were kept in RNA later (Qiagen) at -80°C .

Protein quantification

Quantification of protein was done with the help of the biuret method (Gornall et al. 1949), and the concentration (mg/ml) was determined with the help of a Bovine serum albumin standard curve. This value of protein was used in the calculation of all other biochemical parameters.

Reduced glutathione (GSH) assay

For GSH assay, 100 μl of the supernatant of tissue homogenate was added to 1 ml of 4% w/v sulfosalicylic acid. The

precipitate was formed and the reaction mixture was kept at temperature $2-8^{\circ}\text{C}$ in the refrigerator. After 1 h, samples were centrifuged in a cold centrifuge, i.e., 4°C ; at a rotation of 1200g for 15 min. Pellet was discarded to obtain the supernatant. Furthermore, 100 μl of this supernatant, 2.7 ml of 0.1 M phosphate buffer (pH 8) and 200 μl of 0.1 M 5,5-dithiobis-2-nitrobenzoic acid (DTNB-Ellman's reagent) was mixed to produce a pale yellow color. The color produced was read at 412 nm with the help of a UV-visible spectrophotometer (Perkin Elmer, USA). The calculation was done by applying the molar extinct coefficient of $1.36 \times 10^4 \text{ M}^{-1} \text{ cm}^{-1}$ and results were expressed as μM GSH per mg protein (Jollow et al. 1974).

Catalase assay

Catalase assay was performed by forming a mixture of 50 μl of tissue supernatant and 3 ml H_2O_2 -phosphate buffer (50 mM phosphate buffer, pH adjusted to 7.0, and 12.5 mM hydrogen peroxide- H_2O_2 in the phosphate buffer). Absorbance was read immediately at 240 nm for 2 min at each 60 s. time interval. Absorbance change was determined and results were expressed as μM of H_2O_2 decomposed per min per mg protein (Claiborne 1985).

Superoxide dismutase (SOD) assay

For SOD assay, solution A is made as 50 mM sodium carbonate in 0.1 mM ethylene diamine tetraacetic acid (EDTA) of pH adjusted to 10.8. Solution B consists of 96 mM Nitro blue tetrazolium (NBT) in solution A. Solution C is 20 mM hydroxylamine hydrochloride of pH 6.

Furthermore, the tissue supernatant was added to 2 ml solution B, followed by the addition of 500 μl solution C, which led to auto-oxidation of hydroxylamine hydrochloride. The absorbance was measured at 560 nm at each 30 s. Interval for 2 min and the change in absorbance was noted down. The calculation was done and results were expressed as SOD units per mg protein (Kono 1978).

Glutathione peroxidase (GPX) assay

For the estimation of glutathione peroxidase, a total 2 ml mixture comprising of 1.44 ml of 0.5 M phosphate buffer (pH 7.0), 100 μl of 1 mM EDTA, 100 μl of 1 mM sodium azide, 50 μl of glutathione reductase (1 eu/ml), 100 μl of 1 mM glutathione, 100 μl of 2 mM NADPH, and 10 μl of 0.25 mM hydrogen peroxide (H_2O_2) was made. To this whole mixture, 100 μl of the sample of tissue supernatant was added and absorbance readings were immediately measured at 340 nm for 2 min at each 60 s. interval. Absorbance change was noted down and calculated values were

expressed as nanomoles of oxidized NADPH per min per mg protein (Lawrence and Burk 1976).

Protein carbonylation (PCO) assay

For the estimation of PCO, 20 μ l of dinitrophenylhydrazine (DNPH) was added to 100 μ l of tissue supernatant sample, followed by vortexing. The mixture was left in a dark place for 60 min. Vortexing was done at each 15 min interval. After the final vortexing at 1 h, 120 μ l of 20% trichloroacetic acid (TCA) was added. It was incubated on ice for 15 min. Then, centrifugation was done at 10,000g for 5 min at 4 °C. The supernatant obtained after centrifugation was discarded and the pellet was collected. Pellet was washed twice with 100 μ l of TCA by vortexing and centrifugation in the same way as above. Again, the pellet obtained was washed with 100 μ l of ethyl acetate:ethanol (1:1) mixture by vortexing and centrifugation in the same way as above. Finally, after discarding the supernatant, the pellet was dried for 5 min. The dried pellet was then dispersed in 6 M guanidine. It was then kept for incubation in a shaker at room temperature for 30 min. Absorbance was recorded at 366 nm in a UV–visible spectrophotometer (Colombo et al. 2016). Calculations were done and results were expressed as nanomoles of PCO per mg protein.

Lipid peroxidation (LPO) assay

Malonaldehyde (MDA) is a substance formed as a product of lipid peroxidation which indicates oxidative stress. For the LPO assay, 100 μ l of tissue homogenate supernatant was added to 100 μ l of 0.1 M Tris–HCl (pH 7.4). This mixture was incubated at 37 °C for 2 h. After incubation, 200 μ l of 10% TCA was added to this mixture. Then, centrifugation was done at 1000g for 10 min. 200 μ l of supernatant was collected and, 200 μ l of 0.67% w/v thiobarbituric acid (TBA) was added to it. Furthermore, all the samples were kept in boiling water for 10 min. The pink color was produced. It was cooled followed by the addition of 200 μ l of distilled water. Measurement of absorbance was done at 532 nm on a UV–visible spectrophotometer. Calculations were done and results were expressed as nanomoles of MDA per mg protein (Wills 1966).

Nitrite assay

For nitrite assay, equal volumes, i.e., 100 μ l of tissue homogenate sample, were mixed with 100 μ l of Griess reagent (0.1% naphthyl ethylenediamine dihydrochloride + 1% sulphaniamide in 5% phosphoric acid). This mixture was incubated at 25–30 °C for 10 min in a dark place. Absorbance readings were taken in a UV–visible spectrophotometer at 540 nm. Nitrite concentrations were interpreted from a

standard curve of sodium nitrite solution and results were expressed as μ g of nitrite per mg protein (Green et al. 1982).

Acetylcholinesterase assay

For assessing the activity of acetylcholinesterase, 50 μ l of the tissue sample, 3 ml of 0.01 M sodium phosphate buffer (pH 8), 100 μ l of Ellman's reagent (DTNB), and 100 μ l of acetylthiocholine iodide (AChI) were mixed. Immediately, absorbance was measured at 412 nm every 30 s for 2 min. Results were expressed as μ M of AChI hydrolyzed per min per mg protein (Ellman et al. 1961).

Assessments for mitochondrial complexes

Isolation of mitochondria

Tissue was homogenized in isolation buffer (215 mM mannitol, 75 mM sucrose, 0.1% Bovine serum albumin, and 20 mM HEPES) made in double-distilled water (DDW), pH adjusted to 7.2 by KOH. Centrifugation was done at 10,000g at 4 °C for 5 min. Pellet was collected after discarding the supernatant. The pellet was resuspended in isolation buffer with EGTA and centrifugation was done at 13,000g at 4 °C for 5 min. This process was repeated thrice. The final pellet was resuspended in 1 ml digitonin followed by incubation at room temperature for 10 min. It was again centrifuged at 13,000g for 10 min. In the last step, the pellet was resuspended in isolation buffer without EGTA. This was used for the estimation of mitochondrial complexes (Berman and Hastings 1999).

Mitochondrial complex I activity

NADH dehydrogenase (complex I) activity was determined by forming a mixture of 350 μ l of 0.2 M glycyl glycine buffer, 100 μ l of 10.5 mM Cytochrome-C, 100 μ l of 6 mM NADH, 2.4 ml DDW, and 20 μ l of 0.02 M sodium bicarbonate. 10 μ l isolated mitochondrial sample was added to this mixture. Absorbance was immediately measured in a UV–visible spectrophotometer at each 60 s. interval for 3 min. Change in OD was noted down. Then nanomoles of NADH oxidized per min per mg protein was calculated by applying the values of change in absorbance and extinction coefficient (King and Howard 1967).

Mitochondrial complex II activity

Succinate dehydrogenase (complex II) activity was determined by forming a mixture of 1.5 ml of 0.2 M sodium phosphate buffer (pH 7.8), 200 μ l of 0.6 M succinic acid, 300 μ l of 1% BSA, 25 μ l of 0.03 M potassium ferricyanide, and 1.75 ml of DDW. 25 μ l of mitochondrial sample was added to this mixture and readings were taken

immediately at 420 nm in a UV–visible spectrophotometer at each 60 s interval for 3 min. Calculated values were shown as nanomoles of substrate activity per min per mg protein (King 1967).

Mitochondrial complex III activity (MTT assay)

This assay is also referred to as 3-(4,5-dimethylthiazol-2-yl)-2,5-diphenyl-H-tetrazolium bromide (MTT) assay. 10 µl of MTT was added to 100 µl of the mitochondrial homogenate. It was incubated for 3 h at 37 °C. Here, pale yellow-colored MTT gets converted to formazan crystal. Crystals were solubilized by the addition of a little amount of dimethyl sulfoxide (DMSO-50%). The purple color was produced which was immediately measured at 580 nm wavelength on an ELISA reader (Mosmann 1983; Surin et al. 2017).

Mitochondrial complex IV activity

Cytochrome-C oxidase (complex IV) was estimated by forming a mixture of 100 µl of 0.3 mM reduced Cytochrome-C (reduction was achieved by sodium borohydride crystals, pH adjusted to 7.0 by 100 mM HCl), and 700 µl 75 mM phosphate buffer. 10 µl mitochondrial sample was added to this and absorbance was recorded immediately at 550 nm for 180 s at an interval of every 60 s. Calculations were done and results were expressed as nanomoles of cytochrome-C oxidized per min per mg protein (Sottocasa et al. 1967).

Molecular estimations

Enzyme-linked immunosorbent assay (ELISA)

For the estimation of inflammatory cytokines such as TNF- α , IL-6, and CRP, ELISA was performed only in the hippocampus region as it is the major site for learning and memory.

Tumour necrosis factor- α (TNF- α) TNF- α was estimated in rat hippocampus by Ray Bio rat TNF- α sandwich immunoassay kit (catalog #: ELR-TNFalpha-001). The monoclonal antibody was precoated on the ELISA plate specific for the estimation of TNF- α . 100 µl of the tissue homogenate of the hippocampus was added to each well of the plate. Covered with aluminum foil and incubated for 2.5 h at room temperature. Samples were discarded and washed four times with 300 µl 1 \times wash buffer. 100 µl of 1 \times biotinylated antibody was added and incubated for 1 h. The washing step was repeated as above. Then, 100 µl streptavidin solution was added to the wells, followed by 45 min incubation at room temperature. Washing was repeated. 100 µl 3,3',5,5'-Tetramethylbenzidine (TMB) was added and incubated for 30 min in dark. 50 µl stop solution was added to stop the

reaction and absorbance was recorded at 450 nm on ELISA reader. Results were expressed as pg/ml.

Interleukin-6 (IL-6) Estimation of IL-6 was done by Ray Bio rat IL-6 ELISA kit (catalog #: ELR IL-6-001). According to the instructions of the manufacturer, 100 µl tissue homogenates of the hippocampus were added to each well of the microplate. It was incubated for 1 h room at temperature. The samples were then discarded by washing with 200 µl washing buffer, repeating the same for four times. The plate was tapped on an absorbent paper. Streptavidin solution was pipetted to the wells in a volume of 100 µl. It was kept for incubation for 45 min at room temperature. Washings were repeated. 100 µl TMB one-step substrate reagent was added to the wells, followed by incubation for 30 min at room temperature. 50 µl of stop solution was added to stop the final reaction. Absorbance measurement was done at 450 nm on the ELISA reader. Results were expressed as ng/ml.

C-reactive protein (CRP) CRP was quantified by the Assay-pro rat CRP immunoassay kit (catalog #: ERC1001-1), USA following the manufacturer's instructions. The hippocampus sample in a volume of 50 µl was pipetted to the wells of a microplate. Covered and incubated for 2 h. Then, five-time washings were done with 200 µl wash buffer. The plate was inverted; shook and samples in wells were decanted. 50 µl biotinylated rat CRP antibody was added. Washings were repeated, followed by the addition of 50 µl streptavidin-peroxidase. Incubated for 30 min and washings were repeated in the same way as above. 50 µl of chromogen substrate was added and incubated for 12 min. Finally, 50 µl of stop solution was added and the color was changed from blue to yellow. Absorbance was recorded at 450 nm on ELISA reader. Calculations were done and CRP was expressed as ng/ml.

Quantitative RT-PCR

For the determination of gene expression of IRS-1, PI3-K, AKT, GSK-3 β , BDNF and NF- κ B, q-RT-PCR was performed only in the hippocampus region as it is the major site for learning and memory.

RNA isolation, complementary DNA synthesis, and quantitative RT-PCR The tissue sample of the hippocampus stored at -80 °C was suspended in RNA later for RNA stabilization. (Guerrero et al. 2012). Homogenization of the samples was done in Trizol reagent (Thermo Fisher Scientific, catalog#: 15596026) to extract and isolate RNA from the hippocampus. Chloroform was added to the homogenate to segregate the organic and aqueous layers. After this, isopropanol was added to obtain the RNA from the aqueous phase in the form of a precipitate. Extracted RNA was finally confirmed with the help of gel electrophoresis by running on 1% aga-

rose gel. Quantification of RNA was done by Infinite VRM 200 Pro Nano Quant (Tecan, Switzerland).

cDNA synthesis was done using the RT-first strand synthesis kit (iScript cDNA Synthesis Kit, Bio-rad, catalog#: 170-8891). Here, RNA was reverse transcribed to cDNA with the help of reverse transcriptase.

The primer sequence of genes was designed (Table 1). Expression of different target genes such as IRS-1, PI3K, AKT, GSK-3 β , BDNF, and NF κ B compared to housekeeping control gene β -actin, was determined by qRT-PCR. This was achieved by taking cDNA as a template (Applied Biosystems 7500 Fast Real-Time PCR machine) and with the help of SYBR green (iTaq Universal SYBR Green Supermix, Bio-rad, catalog#: 172-5120). The repeated thermal cycles were set as follows: 95 °C for 10 min. Then, at 95 °C, 40 cycles were repeated followed by 60 °C for 1 min. Calculations were done applying the $2^{-\Delta\Delta C_t}$ formula. Calculated results were shown as fold change or relative gene expression compared to the control group.

Statistical analysis

The average or mean values of each parameter were determined. Standard deviation and standard error mean (SEM) were also calculated. The parameters like escape latency, and biochemical and mitochondrial estimations were analyzed by two-way ANOVA followed by Bonferroni's post hoc test. While, the rest of the parameters like NETQ, TSTQ, DI, CFA, ELISA, and qRT-PCR were analyzed by one-way ANOVA followed by Tukey's test. Data expression was done as mean \pm SEM. All the results were considered to be significantly different if the P value $<$ 0.05.

Results

Effect of CrPic on locomotor activity or closed field activity evaluated by actophotometer

Rearings (Fig. 2a) and ambulations (Fig. 2b) in actophotometer were not significantly changed among various groups.

Table 1 Sequence of forward and reverse primers for the housekeeping gene and target genes

Primer	Forward primer sequence 5'–3'	Reverse primer sequence 5'–3'
β -actin	CCCATCTATGAGGGTTACGC	TTTAATGTCACGCACGATTTTC
IRS-1	CCTTCCCTCTGGGCATGAAA	GACGAGGTAGCTGCGCCAA
PI3-K	AACACAGAAGACCAATACTC	TTCGCCATCTACCACTAC
AKT	TCTATGGCGCTGAGATTGTG	CTTAATGTGCCCGTCTTGT
GSK-3 β	GCATTTATCATTAACTAGCA CCC	ATTTTCTTTCCAAACGTGACC
BDNF	CCGGCTGGTGCAGGAAAG	GGGTAAACCCGATTCCCTGG
NF κ B	ATGGCAGACGATGATCCCTAC	CGGAATCGAAATCCCCTCTGTT

Effect of CrPic on cognitive functions in ICV-STZ rats evaluated by novel object recognition (NOR) and Morris water maze (MWM)

Recognition or associative memory was assessed by NOR. The parameter for the same was the discrimination index (DI). The results showed that in the case of DI, it was significantly less in the ICV-STZ group ($P <$ 0.001) as compared to the normal control group. All three doses of CrPic as well as Riv (2 mg/kg) significantly increased DI ($P <$ 0.001) as compared to the ICV-STZ group (Fig. 3).

Spatial memory was evaluated by determining escape latency in MWM. It was found that there was no significant change on day 1 of the trial phase. However, on days 2, 3, and 4, escape latency was significantly higher in the ICV-STZ group compared to the normal control group ($P <$ 0.001). All the three doses of CrPic (1 mg/kg, 2 mg/kg, 4 mg/kg) and Riv (2 mg/kg) significantly decreased escape latency on day 4 ($P <$ 0.001) (Fig. 4a). The number of entries in the target quadrant (NETQ) was significantly decreased in the ICV-STZ group ($P <$ 0.01) compared to the control

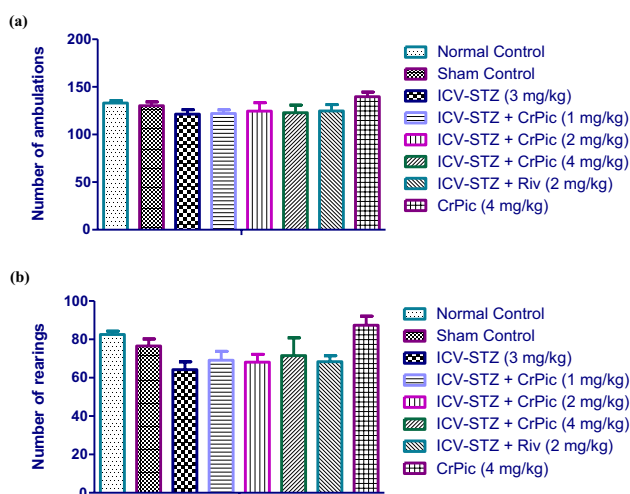


Fig. 2 Effect of CrPic and rivastigmine on **a** ambulation and **b** rearing in actophotometer: analysis of data was done using one-way ANOVA, followed by Tukey's post hoc analysis. All the values were expressed as mean \pm SEM



Fig. 3 Effect of CrPic and rivastigmine on DI: analysis of data was done using one-way ANOVA, followed by Tukey's post hoc analysis. All the values were shown as mean \pm SEM. * $p < 0.05$ as compared to the normal control, # $p < 0.05$ as compared to the ICV-STZ (3 mg/kg)

group. Significantly increased entry ($P < 0.01$) in the target quadrant was observed with CrPic (4 mg/kg) and Riv (2 mg/kg) as compared to the ICV-STZ group (Fig. 4b). Time spent in target quadrant (TSTQ) in ICV-STZ group was found to be significantly decreased ($P < 0.001$) as compared to normal control group, which was again increased ($P < 0.01$) with CrPic (2 mg/kg, 4 mg/kg) and Riv (2 mg/kg) (Fig. 4c).

Effect of CrPic on antioxidant enzymes evaluated by the levels of GSH, catalase, SOD, and GPx

GSH level was significantly lower in the cortex ($P < 0.001$) and hippocampus ($P < 0.01$) regions in ICV-STZ-induced animals as compared to the normal control group. The highest dose of CrPic (4 mg/kg) significantly increased the GSH level in the cortex ($P < 0.01$) and hippocampus ($P < 0.05$) as compared to the ICV-STZ group. Riv (2 mg/kg) also increased the GSH level significantly ($P < 0.001$) in both the regions of the brain (Fig. 5a).

The estimation of catalase revealed significantly diminished catalase activity in cortex ($P < 0.01$) and hippocampus ($P < 0.001$) in the ICV-STZ group as compared to the normal control group. Furthermore, treatment with test and standard drugs did not produce a significant change in catalase activity in the cortex, while the hippocampus region showed a significantly increased level ($P < 0.01$) with Riv (2 mg/kg) treatment (Fig. 5b).

Superoxide dismutase (SOD) activity was found to be significantly decreased ($P < 0.001$) in the ICV-STZ group as compared to the normal group in both the regions of cortex and hippocampus. CrPic (4 mg/kg) and Riv (2 mg/kg) showed significant increase ($P < 0.05$) in SOD level in hippocampus region (Fig. 5c).

The other antioxidant enzyme, glutathione peroxidase (GPX), was found to be significantly decreased ($P < 0.001$) in both the regions of cortex and hippocampus in ICV-STZ rats as compared to the normal control group. Furthermore, the GPX level was significantly elevated ($P < 0.001$) by all the three doses of CrPic as well as Riv (2 mg/kg) in both the respective regions (Fig. 5d).

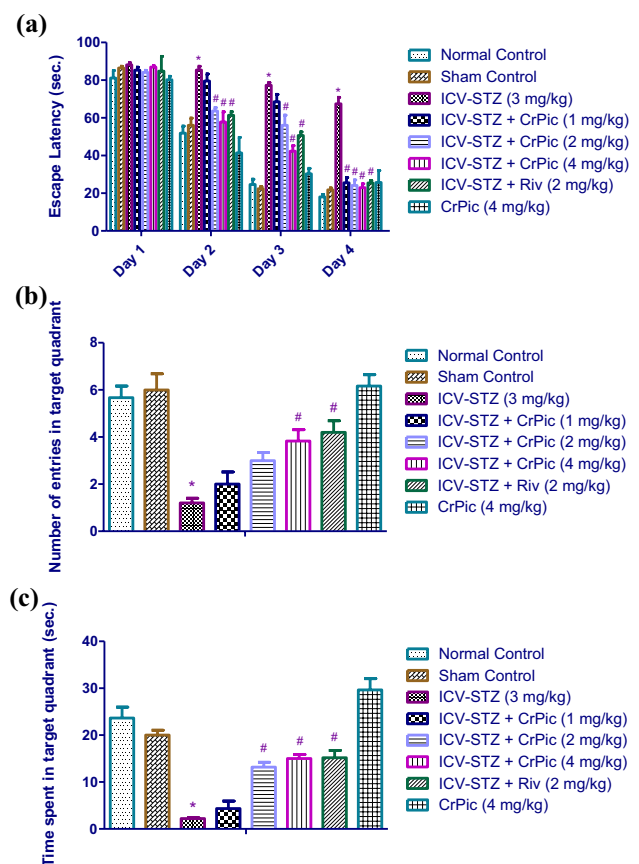


Fig. 4 Effect of CrPic and rivastigmine on **a** escape latency, **b** number of entries in the target quadrant, and **c** time spent in the target quadrant, in MWM: analysis of data for escape latency was done using two-way ANOVA followed by Bonferroni's post hoc analysis and for NETQ/TSTQ, one-way ANOVA followed by Tukey's post hoc analysis was used. All the values were expressed as mean \pm SEM. * $p < 0.05$ as compared to the normal control, # $p < 0.05$ as compared to the ICV-STZ (3 mg/kg)

Effect of CrPic on oxidative and nitrosative stress evaluated by the levels of PCO, MDA, and nitrite

PCO was significantly increased ($P < 0.001$) in the ICV-STZ group in the regions of cortex and hippocampus. CrPic (1 mg/kg and 2 mg/kg) reversed it significantly ($P < 0.05$) as well as CrPic (4 mg/kg), Riv (2 mg/kg) also reduced PCO levels ($P < 0.001$) in cortex and hippocampus (Fig. 6a).

Lipid peroxidation, measured by MDA levels, was significantly increased ($P < 0.001$), in the cortex and hippocampus in the ICV-STZ group compared to the control group. Treatment with different doses of CrPic and Riv (2 mg/kg) significantly attenuated the MDA levels in both the regions except CrPic (1 mg/kg) which did not produce a significant decrease level in the hippocampus (Fig. 6b).

On the other hand, the nitrite level was found to be significantly higher ($P < 0.001$) in the ICV-STZ group as compared to the control group in the cortex and hippocampus

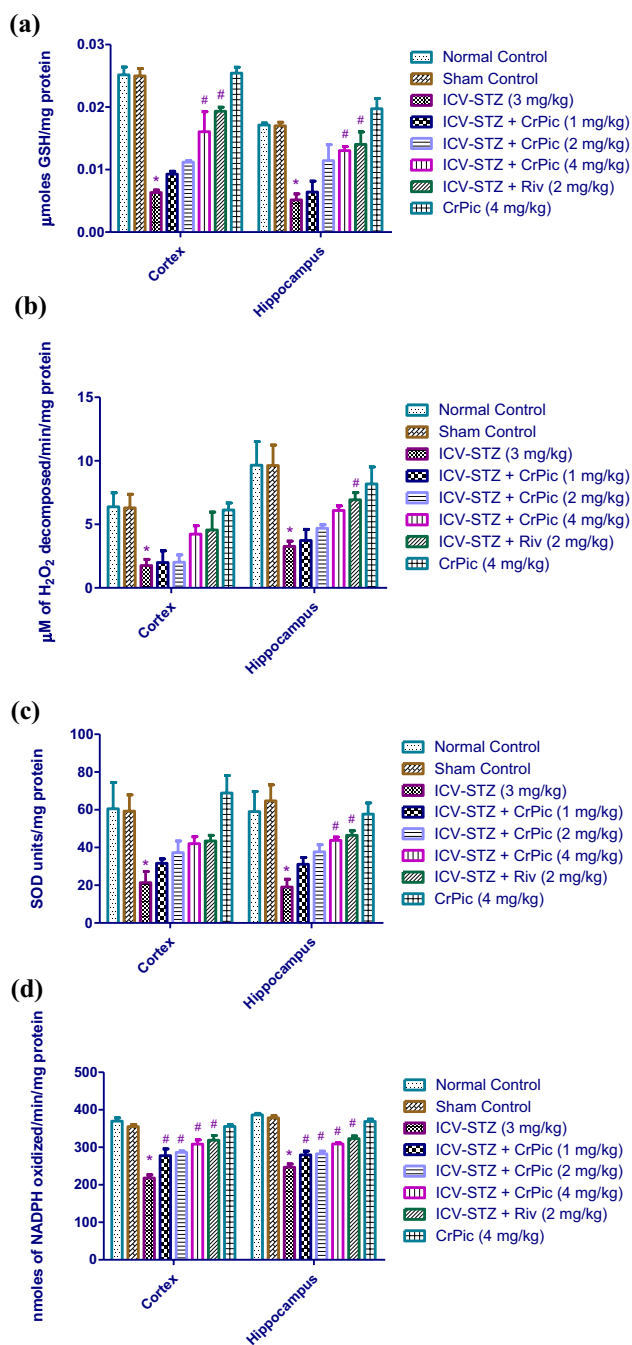


Fig. 5 Effect of CrPic and Rivastigmine on antioxidant system **a** GSH, **b** catalase, **c** SOD, and **d** GPX: analysis of data was done using two-way ANOVA followed by Bonferroni's post hoc analysis. All the values were expressed as mean \pm SEM. * $p < 0.05$ as compared to the normal control, # $p < 0.05$ as compared to the ICV-STZ (3 mg/kg)

regions. Nitrite level was significantly decreased by all three doses of CrPic and Riv (2 mg/kg) in the cortex ($P < 0.001$). CrPic (4 mg/kg) and Riv (2 mg/kg) significantly decreased nitrite levels in the hippocampus as compared to the ICV-STZ group (Fig. 6c).

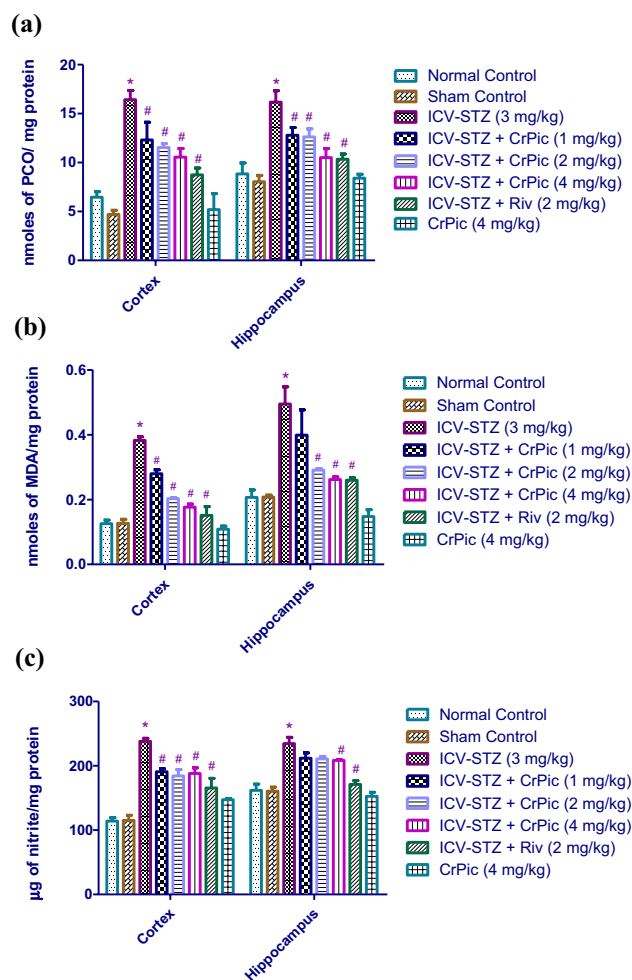


Fig. 6 Effect of CrPic and Rivastigmine on oxidative and nitrosative stress as **a** PCO, **b** MDA, and **c** nitrite: analysis of data was done using Two-way ANOVA followed by Bonferroni's post hoc analysis. All the values were expressed as mean \pm SEM. * $p < 0.05$ as compared to the normal control, # $p < 0.05$ as compared to the ICV-STZ (3 mg/kg)

Effect of CrPic on AchE activity

AchE activity was done to estimate the acetylcholine level. This enzyme is responsible for metabolizing acetylcholine. AchE activity was significantly enhanced in ICV-STZ injected group ($P < 0.001$) in both cortex and hippocampus regions of the brain. None of the doses of CrPic could reverse the AchE activity. However, rivastigmine was found to produce a significant decrease in AchE levels ($P < 0.001$) in the cortex and hippocampus (Fig. 7).

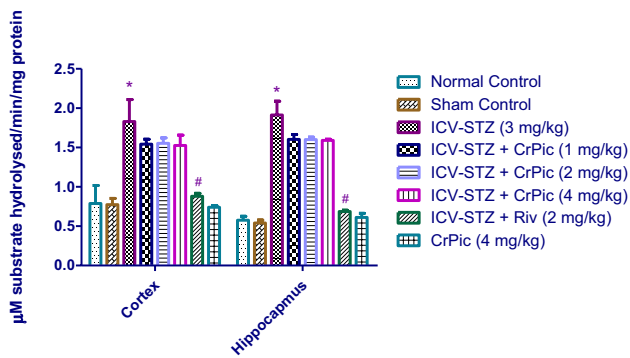


Fig. 7 Effect of CrPic and rivastigmine on acetylcholinesterase (AChE): analysis of data was done using two-way ANOVA followed by Bonferroni's post hoc analysis. All the values were expressed as mean \pm SEM. * $p < 0.05$ as compared to the normal control, # $p < 0.05$ as compared to the ICV-STZ (3 mg/kg)

Effect of CrPic on mitochondrial dysfunction evaluated by the mitochondrial complexes I, II, III, and IV activity

Activities of all the four mitochondrial complexes were significantly decreased ($P < 0.001$) in cortex and hippocampus regions as compared to the control group.

Complex I (Fig. 8a) activity was significantly reversed by the treatment with CrPic (1 mg/kg) ($P < 0.05$), CrPic (2 mg/kg) ($P < 0.01$), CrPic (4 mg/kg) ($P < 0.001$), and Riv (2 mg/kg) (0.001) in the hippocampus region. While, complex II (Fig. 8b) activity was significantly reversed by the treatment with CrPic (2 mg/kg) ($P < 0.01$), CrPic (4 mg/kg) ($P < 0.001$), and Riv (2 mg/kg) (0.001) in the hippocampus region. All the reversals by the treatment were in comparison to the ICV-STZ group. Cortex region did not show a significant difference in complex I and complex II activities.

Treatment with CrPic (2 mg/kg and 4 mg/kg) and Riv 2 mg/kg significantly produced an increase in percentage complex III activity, i.e., MTT assay in the cortex ($P < 0.05$) and hippocampus ($P < 0.001$) regions as compared to the ICV-STZ group (Fig. 8c). Furthermore, complex IV activity was also significantly improved by CrPic (1 mg/kg) ($P < 0.01$) and CrPic (2 mg/kg), CrPic (4 mg/kg), and Riv 2 mg/kg ($P < 0.001$) in cortex and hippocampus as compared to the ICV-STZ group (Fig. 8d).

Effect of CrPic on neuroinflammation evaluated by ELISA of TNF- α , IL-6, and CRP

TNF- α , IL-6, and CRP were evaluated in the hippocampus and results indicated significantly elevated levels of above three markers in the ICV-STZ group ($P < 0.001$) compared to the normal control group.

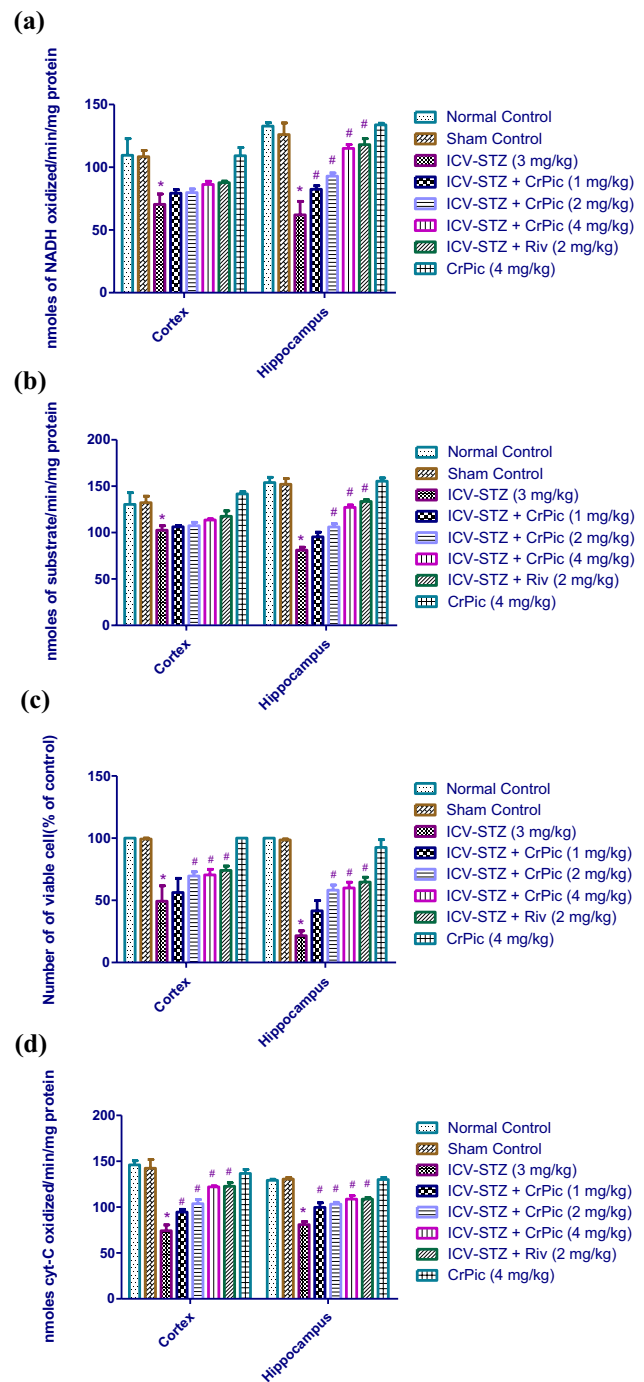


Fig. 8 Effect of CrPic and rivastigmine on mitochondrial dysfunction as **a** complex I, **b** complex II, **c** complex III, and **d** complex IV: analysis of data was done using two-way ANOVA followed by Bonferroni's post hoc analysis. All the values were expressed as mean \pm SEM. * $p < 0.05$ as compared to the normal control, # $p < 0.05$ as compared to the ICV-STZ (3 mg/kg)

However, TNF- α level was decreased significantly with the treatments with CrPic (2 mg/kg) ($P < 0.01$), CrPic (4 mg/kg), and Riv (2 mg/kg) ($P < 0.001$) as compared to ICV-STZ group (Fig. 9a).

CrPic (1 mg/kg) ($P < 0.01$) significantly decreased IL-6 level, while other doses like CrPic (2 mg/kg and 4 mg/kg) and Riv (2 mg/kg) produced even better and improved reversal ($P < 0.001$) (Fig. 9b).

The dose of CrPic (1 mg/kg) ($P < 0.05$), CrPic (2 mg/kg) ($P < 0.01$), CrPic (4 mg/kg), and (Riv 2 mg/kg) ($P < 0.001$) produced significant result in terms of decreasing CRP level in hippocampus as compared to ICV-STZ-induced rats (Fig. 9c).

Effect of CrPic on gene expressions of IRS-1, PI3-K, AKT, GSK-3 β , BDNF, and NF κ B evaluated by qRT-PCR

Gene expression analysis of IRS-1, PI3-K, AKT, GSK-3 β , BDNF, and NF κ B was done in the hippocampus region using qRT-PCR. It was found that expressions of IRS-1 ($P < 0.001$), PI3-K ($P < 0.05$), AKT ($P < 0.01$), and BDNF ($P < 0.001$) genes were significantly decreased, while GSK-3 β ($P < 0.001$) and NF κ B ($P < 0.001$) gene expressions were significantly increased in ICV-STZ group as compared to the normal control group.

Furthermore, the reversal of gene expression of most of the genes was noticed with different doses of CrPic as

compared to ICV-STZ group as follows. Such as IRS-1 gene expression with CrPic (2 mg/kg) ($P < 0.01$), CrPic (4 mg/kg) ($P < 0.001$) (Fig. 10a); PI3-K gene expression with CrPic (4 mg/kg) ($P < 0.01$) (Fig. 10b); AKT gene expression with CrPic (2 mg/kg) ($P < 0.01$), CrPic (4 mg/kg) (0.001) (Fig. 10c); GSK-3 β expression with CrPic (1 mg/kg and 2 mg/kg) ($P < 0.01$), CrPic (4 mg/kg) ($P < 0.001$) (Fig. 10d), BDNF gene expression with (4 mg/kg) ($P < 0.05$) (Fig. 10e), and NF κ B gene expression with CrPic (2 mg/kg and 4 mg/kg) ($P < 0.05$).

Discussion

Intracerebroventricular (ICV) injection of streptozotocin (STZ) leads to brain insulin resistance and mimics pathological and behavioral alterations of human sporadic AD such as cognitive dysfunction, oxidative stress, and mitochondrial dysfunction (Salkovic-Petrisic et al. 2006). Subdiabetogenic dose of ICV-STZ leads to oxidative stress, the release of inflammatory cytokines, mitochondrial dysfunction, and impaired insulin signaling (Labak et al. 2010). As a result, cortex and hippocampus regions of the brain go through insulin signaling impairment, leading to neurodegenerative process, and subsequently, cognitive dysfunction occurs. Hence, ICV-STZ represents a model for sporadic Alzheimer's disease (Labak et al. 2010). The limitation of this model is that, however, ICV-STZ administration in rats produces neuropathological and behavioral disturbances resembling sporadic AD; still, there is not complete resemblance to actual human sporadic AD and clear mechanistic explanations for these phenomena are not established (Grieb 2016).

In the ICV-STZ model, the features of behavioral abnormalities are found in terms of cognitive impairment (Naghizadeh et al. 2013). Our study revealed STZ-induced memory impairment which was assessed by Morris water maze and novel object recognition test. This result is in line with a previous study which demonstrated STZ-induced distortion of recognition or associative memory in novel object recognition test (Espinosa et al. 2013). Treatment with CrPic improved spatial memory in MWM and recognition memory in NOR. There is the least influence of the treatments on the locomotor or exploratory behavior of rats (Sachdeva et al. 2014). This is concurrent with our finding where there were negligible changes in locomotion or closed field activity of diseased and treated animals.

There is a strong link between neuroinflammation and AD pathogenesis involving glial activation (Rai et al. 2014). STZ leads to the formation of neuroinflammatory mediators and free radicals (Rai et al. 2013). Free radicals trigger neuronal damage through the formation of pro-inflammatory

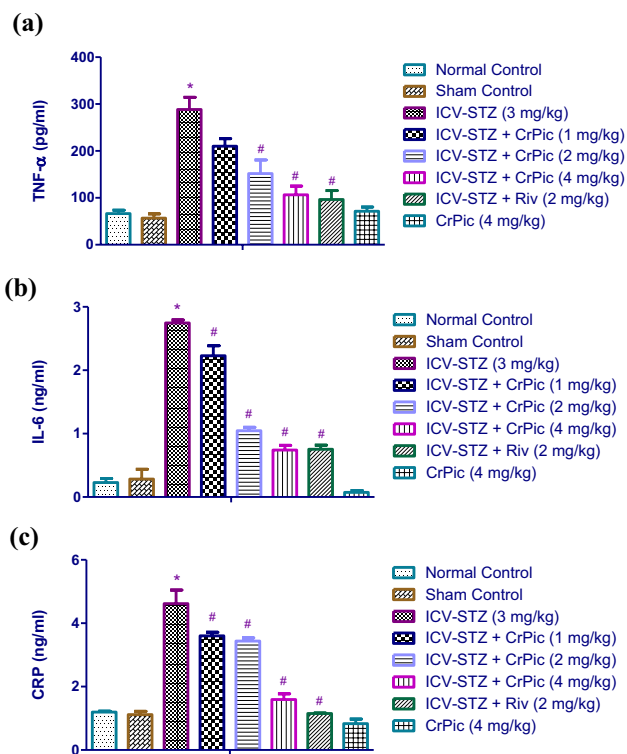


Fig. 9 Effect of CrPic and rivastigmine on **a** TNF- α , **b** IL-6 and **c** CRP: analysis of data was done using one-way ANOVA followed by Tukey's post hoc analysis. All the values were expressed as mean \pm SEM. * $p < 0.05$ as compared to the normal control, # $p < 0.05$ as compared to the ICV-STZ (3 mg/kg)

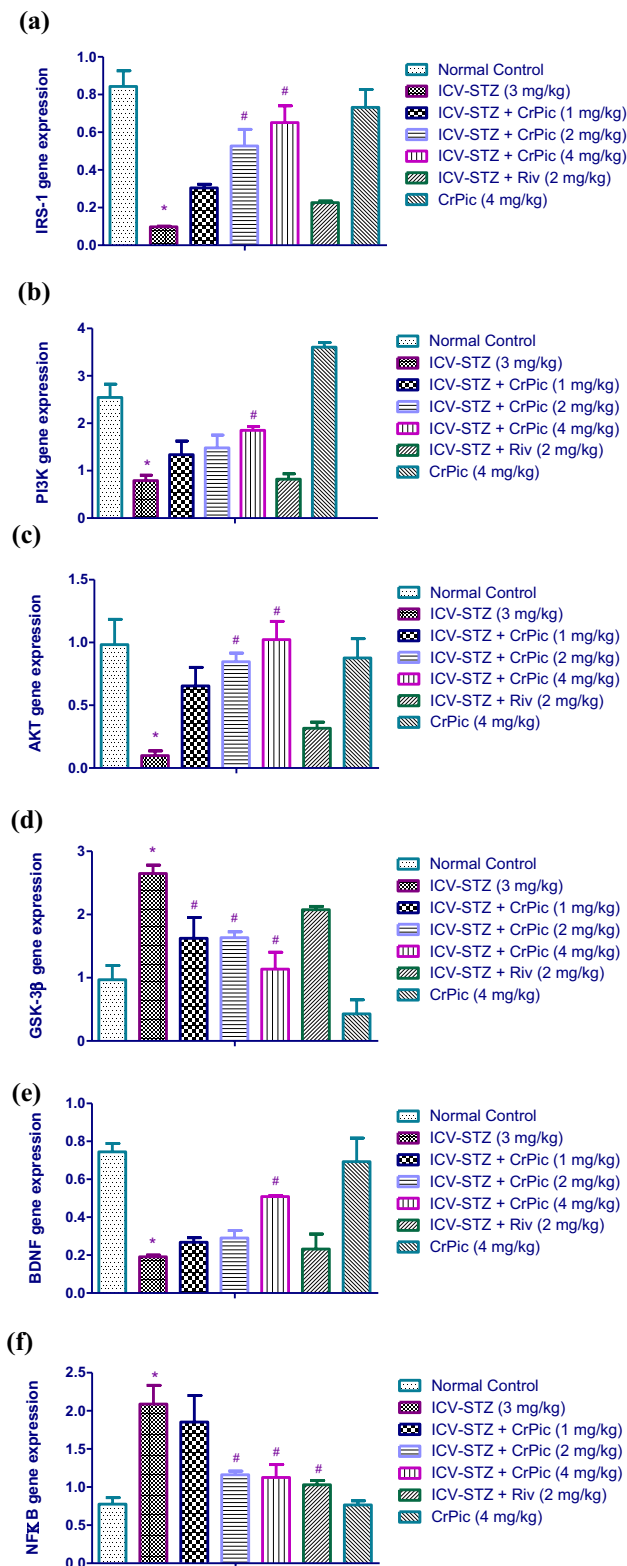


Fig. 10 Effect of CrPic and Rivastigmine on gene expression of **a** IRS-1, **b** PI3K, **c** AKT, **d** GSK-3 β , **e** BDNF, and **f** NF κ B: analysis of data was done using one-way ANOVA, followed by Tukey's post hoc analysis. All the values were expressed as mean \pm SEM. * $p < 0.05$ as compared to the normal control, # $p < 0.05$ as compared to the ICV-STZ (3 mg/kg)

mediators. STZ was found to be responsible for generating reactive oxygen species in the forms of peroxides and superoxides causing oxidative stress. Furthermore, in our study, ICV-STZ decreased levels of antioxidant enzyme system comprising reduced glutathione, catalase, superoxide dismutase, and glutathione peroxidase which were in line with a previous study (Ishrat et al. 2009). The brain is much vulnerable to oxidative stress as it is not as abundant as antioxidant enzymes. Our findings produced significant results showing improved levels of almost all the antioxidant enzymes proving the antioxidant effect CrPic (Sundaram et al. 2013) as well as rivastigmine. Moreover, STZ generates free radicals that react with lipid components of cortex and hippocampus causing lipid peroxidation (Sharma and Gupta 2003). These free radicals also lead to the formation of oxidized adduct products of protein, causing protein carbonylation. Both the phenomenon depict the state of oxidative stress (Ishrat et al. 2009). Furthermore, cognitive impairment has been reported to be induced by brain oxidative damage in the synapses of cortex and hippocampus (Fukui et al. 2002). Our results revealed decreased levels of MDA and protein carbonylation after treatment with CrPic and rivastigmine. This suggests and confirms the oxidative stress neutralizing capacity and protective effect of CrPic against STZ.

Neuronal mitochondrial dysfunction might be the consequence or cause of the generation of reactive oxygen species. This is also one of the key features present in the ICV-STZ model of AD (Saxena et al. 2011). In the present study, the activities of the mitochondrial complexes I, II, III, and IV got reduced. However, the activities of the mitochondrial complexes were enhanced with the treatment of CrPic and rivastigmine. This might be responsible for improved energy metabolism in the brain.

STZ has been reported to aggravate the activity of acetylcholinesterase in the brain leading to cholinergic dysfunction (Biasibetti et al. 2013). The enzyme acetylcholinesterase breaks down acetylcholine, a neurotransmitter having a role in cognition and memory through modulation of synaptic transmission (Bitner et al. 2007). Rivastigmine, which is a cholinesterase inhibitor, causes a decrease in the activity of acetylcholinesterase. However, CrPic could not change its level significantly, indicating that it did not improve cognitive functions through the cholinergic pathway.

Neuroinflammation is the core feature of synaptic dysfunction and neurodegeneration in the ICV-STZ model of AD. STZ causes the release of pro-inflammatory cytokines such as TNF- α and IL-6 through activation of microglia, leading to neuroinflammation (Wang et al. 2012; Rai et al. 2013; Liu et al. 2014; Xiang et al. 2019). Our study revealed modulation of neuroinflammation by CrPic through declined levels of pro-inflammatory cytokines. The possible mechanism for the inhibitory effect of CrPic on the levels of TNF- α , IL-6, and CRP could be mediated partially through

attenuating oxidative stress pathways as well as inhibiting NF κ B pathway (Jain et al. 2007; Selcuk et al. 2012). Rivastigmine also decreased inflammatory cytokines, concurrent with a previous study (Shifrin et al. 2013).

Studies suggest that brain insulin protects the brain against neuroinflammation and oxidative stress-induced neurodegeneration (Kamat 2015). STZ causes disturbances in brain glucose and energy metabolism due to hindered translocation of GLUT 1 and GLUT 3, the main transporters for glucose uptake. Glucose being the major fuel of the brain, loses its existence up to a certain level, leading to neurodegeneration and cognitive impairment (Salkovic-Petrisic et al. 2006).

Furthermore, STZ has been reported to target the genes for IRS-1, PI3K, AKT and GSK-3 β and causes decreased activation of IRS-1, PI3K, AKT, and increased activation of GSK-3 β (Rajasekar et al. 2017a). GSK3- β activation is responsible for tau pathology, a hallmark of the AD model. Decreased activation of PI3K/AKT hinders the translocation of GLUT 1 and GLUT 3 transporter, the main molecule in the uptake of glucose in the brain (Deng et al. 2009). Insulin resistance also leads to dysregulated APP mediated processing of amyloid plaques, another pathological hallmark of AD. Our study has shown that ICV-STZ administered rats produced decreased gene expressions of insulin signaling molecules such as IRS-1, PI3K, AKT, and increased gene expression of GSK-3 β . This dysfunctional insulin signaling in the brain caused by ICV-STZ was found to be improved majorly by the medium and highest doses of CrPic as it increased the gene expression of IRS-1, PI3K, and AKT, and decreased that of GSK-3 β . CrPic increases the binding of insulin to IR. It also increases IRS-1-mediated activation of PI3K and AKT, which leads to decreased activity of GSK-3 β . Moreover, it has been reported to reverse insulin resistance through the IRS-1/PI3K/AKT/GSK-3 β pathway (Morris et al. 2000; Hua et al. 2012). Moreover, ICV-STZ has been found to reduce the level of BDNF (Rajasekar et al. 2017b). CrPic, in this study, elevated the gene expression of BDNF. Hence, CrPic used as a therapeutic intervention was found to reverse ICV-STZ associated neurodegeneration. Furthermore, reports have demonstrated the antioxidant and anti-inflammatory activity of rivastigmine. Yassin et al. (2013) and Karam et al. (2014), concurrent with our results.

Our study demonstrated that, in most of the parameters, the highest dose of CrPic produced close results to the standard drug rivastigmine. It has been reported that PI3K/AKT pathway activation is positively associated with improved cholinergic function and neuronal growth, justifying our results of closely related activities of CrPic and rivastigmine as former is majorly involved in PI3K/AKT activation, while the later enhances cholinergic functions (Omri et al. 2012). The advantage of CrPic over rivastigmine can be counted as its easy availability and exclusion of cholinergic side effects.

Moreover, CrPic can be included in dietary supplements and drinking water.

However, the major limitation of this study is that mainstream pathological hallmarks of AD were not estimated. Still, in the present study, CrPic was found to attenuate cognitive deficit induced by ICV-STZ by targeting the insulin signaling pathway of IRS-1/PI3K/AKT/GSK-3 β as well as reversing oxidative stress, mitochondrial dysfunction, and neuroinflammation.

For future study, human equivalent dose of CrPic of the treated rats as a possible therapeutic agent in treatment of AD could maximally be 0.64 mg/kg, calculated according to a previously reported dose conversion study (Nair and Jacob 2016).

Conclusion

In a nutshell, this study can be concluded that in most of the behavioral, biochemical, and molecular parameters, the medium dose (2 mg/kg) and highest dose (4 mg/kg) of CrPic were found to be more effective than the lowest dose (1 mg/kg). It reversed some of the core features of the sporadic AD model such as oxidative stress, neuroinflammation, and mitochondrial dysfunction in the regions of cortex and hippocampus. Moreover, CrPic ameliorated STZ-induced central insulin resistance by targeting the IRS-1/PI3K/AKT/GSK-3 β pathway of insulin signaling. This leads to improved cognition and memory in ICV-STZ-induced rat model of AD.

Acknowledgements University Grants Commission, New Delhi is acknowledged for granting the funds for the conduct of the research work. The letter-number for providing funds is F1-17.1/2015-16/MANF-2015-17-BIH-72699.

Compliance with ethical standards

Conflict of interest The authors declare that there were no conflicts of interest.

References

- Anderson RA, Bryden NA, Polansky MM, Gautschi K (1996) Dietary chromium effects on tissue chromium concentrations and chromium absorption in rats. *J Trace Elem Exp Med* 9:11–25
- Anderson RA, Roussel A-M, Zouari N, Mahjoub S, Matheau J-M, Kerkeni A (2001) Potential antioxidant effects of zinc and chromium supplementation in people with type 2 diabetes mellitus. *J Am Coll Nutr* 20:212–218
- Antunes M, Biala G (2012) The novel object recognition memory: neurobiology, test procedure, and its modifications. *Cogn Process* 13:93–110

- Baki L, Shioi J, Wen P, Shao Z, Schwarzman A, Gama-Sosa M, Neve R, Robakis NK (2004) PS1 activates PI3K thus inhibiting GSK-3 activity and tau overphosphorylation: effects of FAD mutations. *EMBO J* 23:2586–2596
- Berman SB, Hastings TG (1999) Dopamine oxidation alters mitochondrial respiration and induces permeability transition in brain mitochondria: implications for Parkinson's disease. *J Neurochem* 73:1127–1137
- Biasibetti R, Tramontina AC, Costa AP, Dutra MF, Quincozes-Santos A, Nardin P, Bernardi CL, Wartchow KM, Lunardi PS, Gonçalves C-A (2013) Green tea (–) epigallocatechin-3-gallate reverses oxidative stress and reduces acetylcholinesterase activity in a streptozotocin-induced model of dementia. *Behav Brain Res* 236:186–193
- Bitner RS, Bunnelle WH, Anderson DJ, Briggs CA, Buccafusco J, Curzon P, Decker MW, Frost JM, Gronlien JH, Gubbins E (2007) Broad-spectrum efficacy across cognitive domains by $\alpha 7$ nicotinic acetylcholine receptor agonism correlates with activation of ERK1/2 and CREB phosphorylation pathways. *J Neurosci* 27:10578–10587
- Claiborne A (1985) Handbook of methods for oxygen radical research. CRC Press, Boca Raton
- Colombo G, Clerici M, Garavaglia ME, Giustarini D, Rossi R, Milzani A, Dalle-Donne I (2016) A step-by-step protocol for assaying protein carbonylation in biological samples. *J Chromatogr B* 1019:178–190
- de la Monte SM (2012) Brain insulin resistance and deficiency as therapeutic targets in Alzheimer's disease. *Curr Alzheimer Res* 9:35–66
- Del Pino J, Zeballos G, Anadón MJ, Moyano P, Díaz MJ, García JM, Frejo MT (2016) Cadmium-induced cell death of basal forebrain cholinergic neurons mediated by muscarinic M1 receptor blockade, increase in GSK-3 β enzyme, β -amyloid and tau protein levels. *Arch Toxicol* 90:1081–1092
- Deng Y, Li B, Liu Y, Iqbal K, Grundke-Iqbal I, Gong C-X (2009) Dysregulation of insulin signaling, glucose transporters, O-GlcNAcylation, and phosphorylation of tau and neurofilaments in the brain: Implication for Alzheimer's disease. *Am J Pathol* 175:2089–2098
- Desbois-Mouthon C, Cadoret A, Blivet-Van Eggelpeol M-J, Bertrand F, Cherqui G, Perret C, Capeau J (2001) Insulin and IGF-1 stimulate the β -catenin pathway through two signalling cascades involving GSK-3 β inhibition and Ras activation. *Oncogene* 20:252
- Dubey VK, Ansari F, Vohora D, Khanam R (2015) Possible involvement of corticosterone and serotonin in antidepressant and anti-anxiety effects of chromium picolinate in chronic unpredictable mild stress induced depression and anxiety in rats. *J Trace Elem Med Biol* 29:222–226
- Ellman GL, Courtney KD, Andres V Jr, Featherstone RM (1961) A new and rapid colorimetric determination of acetylcholinesterase activity. *Biochem Pharmacol* 7:88–95
- Espinosa J, Rocha A, Nunes F, Costa MS, Schein V, Kazlauckas V, Kalinine E, Souza DO, Cunha RA, Porciúncula LO (2013) Caffeine consumption prevents memory impairment, neuronal damage, and adenosine A 2A receptors upregulation in the hippocampus of a rat model of sporadic dementia. *J Alzheimer's Dis* 34:509–518
- Franklin M, Odontiadis J (2003) Effects of treatment with chromium picolinate on peripheral amino acid availability and brain monoamine function in the rat. *Pharmacopsychiatry* 36:176–180
- Frölich L, Blum-Degen D, Riederer P, Hoyer S (1999) A disturbance in the neuronal insulin receptor signal transduction in sporadic Alzheimer's disease. *Ann N Y Acad Sci* 893:290–293
- Fukui K, Omoi NO, Hayasaka T, Shinnkai T, Suzuki S, Abe K, Urano S (2002) Cognitive impairment of rats caused by oxidative stress and aging, and its prevention by vitamin E. *Ann N Y Acad Sci* 959:275–284
- Gornall AG, Bardawill CJ, David MM (1949) Determination of serum proteins by means of the biuret reaction. *J Biol Chem* 177:751–766
- Green LC, Wagner DA, Glogowski J, Skipper PL, Wishnok JS, Tannenbaum SR (1982) Analysis of nitrate, nitrite, and [¹⁵N] nitrate in biological fluids. *Anal Biochem* 126:131–138
- Grieb P (2016) Intracerebroventricular streptozotocin injections as a model of Alzheimer's disease: in search of a relevant mechanism. *Mol Neurobiol* 53:1741–1752
- Guerrero L, Castillo J, Quiñones M, Garcia-Vallvé S, Arola L, Pujadas G, Muguerza B (2012) Inhibition of angiotensin-converting enzyme activity by flavonoids: structure-activity relationship studies. *PLoS ONE* 7:e49493
- Hua Y, Clark S, Ren J, Sreejayan N (2012) Molecular mechanisms of chromium in alleviating insulin resistance. *J Nutr Biochem* 23:313–319
- Ishrat T, Parveen K, Khan MM, Khuwaja G, Khan MB, Yousuf S, Ahmad A, Shrivastav P, Islam F (2009) Selenium prevents cognitive decline and oxidative damage in rat model of streptozotocin-induced experimental dementia of Alzheimer's type. *Brain Res* 1281:117–127
- Jain SK, Rains JL, Croad JL (2007) Effect of chromium niacinate and chromium picolinate supplementation on lipid peroxidation, TNF- α , IL-6, CRP, glycated hemoglobin, triglycerides, and cholesterol levels in blood of streptozotocin-treated diabetic rats. *Free Radical Biol Med* 43:1124–1131
- Jollow D, Mitchell J, Zampaglione NA, Gillette J (1974) Bromobenzene-induced liver necrosis. Protective role of glutathione and evidence for 3,4-bromobenzene oxide as the hepatotoxic metabolite. *Pharmacology* 11:151–169
- Kamat PK (2015) Streptozotocin induced Alzheimer's disease like changes and the underlying neural degeneration and regeneration mechanism. *Neural Regen Res* 10:1050
- Karam A, Nadia A, Abd E, Nemat A, Siham M (2014) Protective effect of ginger (*Zingiber officinale*) on Alzheimer's disease induced in rats. *J Neuroinfect Dis* 5:2
- King TE (1967) Preparation of succinate dehydrogenase and reconstitution of succinate oxidase, methods in enzymology. Elsevier, Amsterdam, pp 322–331
- King TE, Howard RL (1967) Preparations and properties of soluble NADH dehydrogenases from cardiac muscle, methods in enzymology. Elsevier, Amsterdam, pp 275–294
- Kono Y (1978) Generation of superoxide radical during autoxidation of hydroxylamine and an assay for superoxide dismutase. *Arch Biochem Biophys* 186:189–195
- Labak M, Foniok T, Kirk D, Rushforth D, Tomanek B, Jasiński A, Grieb P (2010) Metabolic changes in rat brain following intracerebroventricular injections of streptozotocin: a model of sporadic Alzheimer's disease, Brain Edema XIV. Springer, New York, pp 177–181
- Lawrence RA, Burk RF (1976) Glutathione peroxidase activity in selenium-deficient rat liver. *Biochem Biophys Res Commun* 71:952–958
- Liu M, Liao K, Yu C, Li X, Liu S, Yang S (2014) Puerarin alleviates neuropathic pain by inhibiting neuroinflammation in spinal cord. *Mediat Inflamm* 2014:1–9
- Martin J, Wang ZQ, Zhang XH, Wachtel D, Volaufova J, Matthews DE, Cefalu WT (2006) Chromium picolinate supplementation attenuates body weight gain and increases insulin sensitivity in subjects with type 2 diabetes. *Diabetes Care* 29:1826–1832
- Morris R (1984) Developments of a water-maze procedure for studying spatial learning in the rat. *J Neurosci Methods* 11:47–60
- Morris RG, Garrud P, Rawlins JA, O'Keefe J (1982) Place navigation impaired in rats with hippocampal lesions. *Nature* 297:681

- Morris B, Kouta S, Robinson R, MacNeil S, Heller S (2000) Chromium supplementation improves insulin resistance in patients with type 2 diabetes mellitus. *Diabet Med* 17:684–685
- Mosmann T (1983) Rapid colorimetric assay for cellular growth and survival: application to proliferation and cytotoxicity assays. *J Immunol Methods* 65:55–63
- Mozaffari MS, Patel C, Ballas C, Schaffer SW (2005) Effects of chronic chromium picolinate treatment in uninephrectomized rat. *Metabolism* 54:1243–1249
- Naghizadeh B, Mansouri M, Ghorbanzadeh B, Farbood Y, Sarkaki A (2013) Protective effects of oral crocin against intracerebroventricular streptozotocin-induced spatial memory deficit and oxidative stress in rats. *Phytomedicine* 20:537–542
- Nair AB, Jacob S (2016) A simple practice guide for dose conversion between animals and human. *J Basic Clin Pharm* 7:27
- Omri AE, Han J, Kawada K, Abdrabbah MB, Isoda H (2012) Luteolin enhances cholinergic activities in PC12 cells through ERK1/2 and PI3K/Akt pathways. *Brain Res* 1437:16–25
- Onor M, Trevisiol M, Negro C, Aguglia E (2006) Different perception of cognitive impairment, behavioral disturbances, and functional disabilities between persons with mild cognitive impairment and mild Alzheimer's disease and their caregivers. *Am J Alzheimer's Dis Other Dement* 21:333–338
- Rai S, Kamat PK, Nath C, Shukla R (2013) A study on neuroinflammation and NMDA receptor function in STZ (ICV) induced memory impaired rats. *J Neuroimmunol* 254:1–9
- Rai S, Kamat PK, Nath C, Shukla R (2014) Glial activation and post-synaptic neurotoxicity: the key events in Streptozotocin (ICV) induced memory impairment in rats. *Pharmacol Biochem Behav* 117:104–117
- Rajasekar N, Nath C, Hanif K, Shukla R (2017a) Intranasal insulin administration ameliorates streptozotocin (ICV)-induced insulin receptor dysfunction, neuroinflammation, amyloidogenesis, and memory impairment in rats. *Mol Neurobiol* 54:6507–6522
- Rajasekar N, Nath C, Hanif K, Shukla R (2017b) Intranasal insulin improves cerebral blood flow, Nrf-2 expression and BDNF in STZ (ICV)-induced memory impaired rats. *Life Sci* 173:1–10
- Sachdeva AK, Kuhad A, Chopra K (2014) Naringin ameliorates memory deficits in experimental paradigm of Alzheimer's disease by attenuating mitochondrial dysfunction. *Pharmacol Biochem Behav* 127:101–110
- Sahin K, Tuzcu M, Orhan C, Gencoglu H, Ulas M, Atalay M, Sahin N, Hayirli A, Komorowski JR (2012) The effects of chromium picolinate and chromium histidinate administration on NF- κ B and Nrf2/HO-1 pathway in the brain of diabetic rats. *Biol Trace Elem Res* 150:291–296
- Salkovic-Petrisic M, Tribl F, Schmidt M, Hoyer S, Riederer P (2006) Alzheimer-like changes in protein kinase B and glycogen synthase kinase-3 in rat frontal cortex and hippocampus after damage to the insulin signalling pathway. *J Neurochem* 96:1005–1015
- Sargent L, Brown R (2017) Assessing the current state of cognitive frailty: measurement properties. *J Nutr Health Aging* 21:152–160
- Saxena G, Patro IK, Nath C (2011) ICV STZ induced impairment in memory and neuronal mitochondrial function: a protective role of nicotinic receptor. *Behav Brain Res* 224:50–57
- Selcuk MY, Aygen B, Dogukan A, Tuzcu Z, Akdemir F, Komorowski JR, Atalay M, Sahin K (2012) Chromium picolinate and chromium histidinate protects against renal dysfunction by modulation of NF- κ B pathway in high-fat diet fed and Streptozotocin-induced diabetic rats. *Nutr Metab* 9:30
- Sharma M, Gupta Y (2002) Chronic treatment with trans resveratrol prevents intracerebroventricular streptozotocin induced cognitive impairment and oxidative stress in rats. *Life Sci* 71:2489–2498
- Sharma M, Gupta Y (2003) Effect of alpha lipoic acid on intracerebroventricular streptozotocin model of cognitive impairment in rats. *Eur Neuropsychopharmacol* 13:241–247
- Shifrin H, Nadler-Milbauer M, Shoham S, Weinstock M (2013) Rivastigmine alleviates experimentally induced colitis in mice and rats by acting at central and peripheral sites to modulate immune responses. *PLoS ONE* 8:e57668
- Sottocasa GL, Kuylenstierna B, Ernster L, Bergstrand A (1967) An electron-transport system associated with the outer membrane of liver mitochondria: a biochemical and morphological study. *J Cell Biol* 32:415–438
- Steen E, Terry BM, Rivera JE, Cannon JL, Neely TR, Tavares R, Xu XJ, Wands JR, de la Monte SM (2005) Impaired insulin and insulin-like growth factor expression and signaling mechanisms in Alzheimer's disease—is this type 3 diabetes? *J Alzheimer's Dis* 7:63–80
- Sundaram B, Aggarwal A, Sandhir R (2013) Chromium picolinate attenuates hyperglycemia-induced oxidative stress in streptozotocin-induced diabetic rats. *J Trace Elem Med Biol* 27:117–121
- Surin A, Sharipov R, Krasil'nikova I, Boyarkin D, Lisina OY, Gorbacheva L, Avetisyan A, Pinelis V (2017) Disruption of functional activity of mitochondria during MTT assay of viability of cultured neurons. *Biochemistry (Moscow)* 82:737–749
- Talbot K, Wang H-Y, Kazi H, Han L-Y, Bakshi KP, Stucky A, Fuino RL, Kawaguchi KR, Samoyedny AJ, Wilson RS (2012) Demonstrated brain insulin resistance in Alzheimer's disease patients is associated with IGF-1 resistance, IRS-1 dysregulation, and cognitive decline. *J Clin Investig* 122:1316–1338
- Wang T, Fu F, Han B, Zhang L, Zhang X (2012) Danshensu ameliorates the cognitive decline in streptozotocin-induced diabetic mice by attenuating advanced glycation end product-mediated neuroinflammation. *J Neuroimmunol* 245:79–86
- Wills E (1966) Mechanisms of lipid peroxide formation in animal tissues. *Biochem J* 99:667
- Xiang Y, Liu C, Han L (2019) Apelin-13 suppresses neuroinflammation against cognitive deficit in a streptozotocin-induced rat model of Alzheimer's disease through activation of BDNF-TrkB signaling pathway. *Front Pharmacol* 10:395
- Yassin N, El-Shenawy S, Mahdy KA, Gouda N, Marrie A, Farrag A, Ibrahim BM (2013) Effect of *Boswellia serrata* on Alzheimer's disease induced in rats. *J Arab Soc Med Res* 8:1–11

Publisher's Note Springer Nature remains neutral with regard to jurisdictional claims in published maps and institutional affiliations.